J Antimicrob Chemother
https://doi.org/10.1093/jac/dkac257

Journal of Antimicrobial Chemotherapy

Efficacy of ensitrelvir against SARS-CoV-2 in a delayed-treatment mouse model

Haruaki Nobori [1], Keita Fukao[1], Takayuki Kuroda[1], Naomi Anan[1], Ryoichi Tashima[1], Masaaki Nakashima[1], Sayuri Noda[1], Minako Tajiri[1], Mikinori Torii[1], Shinsuke Toba[1,2], Kentaro Uemura[1,2,3], Takao Sanaki [1], Takao Shishido[1], Yuki Tachibana [1] and Teruhisa Kato [1]*

[1]Pharmaceutical Research Division, Shionogi & Co., Ltd., 1-1, Futaba-cho 3-chome, Toyonaka, Osaka 561-0825, Japan; [2]Division of Molecular Pathobiology, International Institute for Zoonosis Control, Hokkaido University, Kita-20, Nishi-10 Kita-ku, Sapporo, Hokkaido 001-0020, Japan; [3]Laboratory of Biomolecular Science, Faculty of Pharmaceutical Sciences, Hokkaido University, Kita-12, Nishi-6 Kita-ku, Sapporo, Hokkaido 060-0812, Japan

*Corresponding author. E-mail: teruhisa.kato@shionogi.co.jp

Received 28 March 2022; accepted 6 July 2022

Objectives: Severe acute respiratory syndrome coronavirus 2 (SARS-CoV-2) is the aetiological agent of coronavirus disease 2019 (COVID-19) and a devastating worldwide health concern. Development of safe and effective treatments is not only important for interventions during the current pandemic, but also for providing general treatment options moving forward. We have developed ensitrelvir, an antiviral compound that targets the 3C-like protease of SARS-CoV-2. In this study, a delayed-treatment mouse model was used to clarify the potential *in vivo* efficacy of ensitrelvir.

Methods: Female BALB/cAJcl mice of different ages were infected with the SARS-CoV-2 gamma strain (hCoV-19/Japan/TY7-501/2021) or mouse-adapted SARS-CoV-2 MA-P10 and then 24 h post-infection orally administered various doses of ensitrelvir or vehicle. Viral titres and RNA levels in the lungs were quantified using VeroE6/TMPRSS2 cells and RT–qPCR, respectively. Body weight loss, survival, lung weight, cytokine/chemokine production, nucleocapsid protein expression and lung pathology were evaluated to investigate the *in vivo* efficacy of ensitrelvir.

Results: Based on infectious viral titres and viral RNA levels in the lungs of infected mice, ensitrelvir reduced viral loads in a dose-dependent manner. The antiviral efficacy correlated with increased survival, reduced body weight loss, reduced pulmonary lesions and suppression of inflammatory cytokine/chemokine levels.

Conclusions: This was the first evaluation of the *in vivo* anti-SARS-CoV-2 efficacy of ensitrelvir in a delayed-treatment mouse model. In this model, ensitrelvir demonstrated high antiviral potential and suppressed lung inflammation and lethality caused by SARS-CoV-2 infection. The findings support the continued clinical development of ensitrelvir as an antiviral agent to treat patients with COVID-19.

Introduction

Severe acute respiratory syndrome coronavirus 2 (SARS-CoV-2), the aetiological agent of coronavirus disease 2019 (COVID-19), was first identified in Wuhan, Hubei Province, People's Republic of China in December 2019. The WHO declared the SARS-CoV-2 outbreak a Public Health Emergency of International Concern on 30 January 2020 and subsequently a pandemic on 11 March 2020. COVID-19 remains a global health crisis with over 455 million confirmed cases and over 6 million reported deaths worldwide as of 15 March 2022,[1] demonstrating the critical need for effective vaccines and therapeutics to combat SARS-CoV-2.

COVID-19 is more likely to be severe in high-risk patients, including those with advanced age, cardiovascular disease, respiratory disease, renal disease, diabetes mellitus, obesity or immunodeficiency. Such patients present with rapidly progressive pneumonia, accompanied by symptoms including shortness of breath and dyspnoea, and may require supplemental oxygen and even mechanical ventilation or extracorporeal membrane oxygenation. Severe COVID-19 disease is also characterized by thromboembolic disease and exhibits high mortality. The pandemic has led to severe pressure on and collapse of healthcare systems worldwide.[2] Development of vaccines against SARS-CoV-2 is an important strategy for preventing infection and transmission. However, the identification and development

of antiviral agents to treat SARS-CoV-2 infections and prevent disease progression are also critical, especially in regard to breakthrough infections, unvaccinated individuals and situations in which the target pathogen is continually changing antigenically. Much of the initial effort aimed at identifying effective antivirals against COVID-19 has focused on identifying existing drugs for repurposing by screening their antiviral activity against SARS-CoV-2 *in vitro*. Unfortunately, this strategy has had limited success with frequent conflicting clinical outcomes.[3]

Vaccination against SARS-CoV-2 is being promoted throughout the world. However, some spike-protein mutations enhance virus infectivity and pathogenicity and allow the virus to evade host immune surveillance. Therefore, SARS-CoV-2 may continue to be a problematic health issue. Accordingly, the development of new anti-SARS-CoV-2 therapeutic agents is highly desirable. Ensitrelvir (formerly S-217622) is a candidate compound that has been developed for the treatment of patients with COVID-19 and is an inhibitor of the SARS-CoV-2 3C-like (3CL) protease.[4] Ensitrelvir has been shown to exhibit *in vitro* efficacy against various SARS-CoV-2 variants, including alpha, beta, gamma, delta and omicron strains, and demonstrates *in vivo* efficacy in mice when administered immediately after SARS-CoV-2 infection.[4] The current study evaluated the inhibitory effect of ensitrelvir on SARS-CoV-2 replication in mice using a delayed-treatment model. Mice infected with a gamma or mouse-adapted strain of SARS-CoV-2 were administered ensitrelvir or vehicle 24 h post-infection. The findings should provide valuable insight into the *in vivo* efficacy of ensitrelvir in a model system using kinetics of intervention representative of real-world clinical settings.

Materials and methods

Ethics

The study complied with the Standards for the Reliability of Application Data (Article 43, Enforcement Regulations, Law for the Assurance of Quality, Efficacy, and Safety of Pharmaceuticals and Medical Devices). The animal protocols were approved by the Shionogi Pharmaceutical Research Centre Institute Director (Shionogi & Co., Ltd., Toyonaka, Japan) based on the report of the Institutional Animal Care and Use Committee (Approval No. S21140D-0001 and S21068D-0008). The animal facilities were accredited by the Association for Assessment and Accreditation of Laboratory Animal Care (AAALAC) International.

Cell line and SARS-CoV-2 viruses

Transmembrane serine protease 2 (TMPRSS-2)-expressing Vero E6 (VeroE6/TMPRSS2) cells[5] were obtained from the Japanese Collection of Research Bioresources Cell Bank (Osaka, Japan) and maintained in DMEM (Thermo Fisher Scientific, Waltham, MA, USA) containing 10% heat-inactivated FBS (Sigma–Aldrich, St. Louis, MO, USA) and 1% penicillin-streptomycin solution (Thermo Fisher Scientific). The SARS-CoV-2 gamma strain (hCoV-19/Japan/TY7-501/2021, Pango lineage P.1) was obtained from the National Institute of Infectious Diseases, Tokyo, Japan. The SARS-CoV-2 MA-P10 strain (mouse-adapted hCoV-19/Japan/TY/WK-521/2020, Pango lineage A)[6] was obtained from the Division of Molecular Pathobiology, International Institute for Zoonosis Control, Hokkaido University, Sapporo, Japan. The viruses were propagated in VeroE6/TMPRSS2 cells to prepare virus stocks, which were stored at −80°C. Viral titres were determined in VeroE6/TMPRSS2 cells using $TCID_{50}$ assays.

Animals

Female BALB/cAJcl mice were obtained from CLEA Japan, Inc. (Tokyo, Japan). All mice were maintained in a controlled environment of 20°C–26°C and 30%–70% relative humidity with a 12 h light/dark cycle. Mice were housed 4–5 per cage with a standard chow diet of CE-2 (CLEA Japan, Inc.) and water was available *ad libitum*. Frozen virus stocks were diluted with Dulbecco's PBS (DPBS; Thermo Fisher Scientific) to prepare suspensions of 2.00×10^5 or 2.00×10^6 $TCID_{50}$/mL for the gamma strain and 6.00×10^4 $TCID_{50}$/mL for MA-P10. The mice were intranasally inoculated under anaesthesia at 5, 20 or 40 weeks of age with 50 μL of virus suspension per mouse. The animals were subsequently treated as described. Mice with >20% loss of initial body weight were euthanized, according to humane endpoints.

Ensitrelvir preparation and dosing

The anti-SARS-CoV-2 test compound of ensitrelvir was used as an ensitrelvir–fumaric acid co-crystal ($C_{22}H_{17}ClF_3N_9O_2{\cdot}C_4H_4O_4$; Shionogi & Co. Ltd., Osaka, Japan) and freshly prepared in 0.5% (w/v) methylcellulose 400 cP (MC) solution (Fujifilm Wako Pure Chemical Corp., Osaka, Japan). According to a previous report,[4] the ensitrelvir was orally administered twice daily, every 12 h, for 2, 3 or 5 days, as indicated, starting 24 h post-infection. The ensitrelvir was dosed at 0, 4, 8, 16, 32 or 64 mg (free-form mass)/kg of body weight, as indicated, in dosage volumes of 10 mL/kg of body weight.

Lung specimen/tissue collection and lung homogenate preparation

Mice ($n=3$–5 per group) were euthanized 1, 2, 3 or 4 days post-infection and their lungs removed. After homogenization of the lung samples with 2 mL of DPBS, the homogenates were centrifuged at 1750×g for 5 min at 4°C and filtered through a 0.45 μm filter. Homogenate aliquots were stored at −80°C until use.

Viral titre and RNA analysis

VeroE6/TMPRSS2 stocks were thawed and passaged several times in complete DMEM in 5% CO_2 at 37°C. Seventy-five microlitres of viral assay medium consisting of MEM (Thermo Fisher Scientific) supplemented with 2% heat-inactivated FBS and 1% penicillin-streptomycin was added to the wells of 96-well plates. The cells were diluted to 1.5×10^5 cells/mL with viral assay medium and then seeded at 100 μL/well. Lung homogenates were serially diluted with viral assay medium. Twenty-five microlitres of the diluted samples was added to the wells and the plates then incubated in 5% CO_2 at 37°C for 4 days. After incubation, virus-induced cytopathic effect (CPE) was evaluated under a microscope. Viral titres were expressed as $\log_{10}$ $TCID_{50}$/mL. If no CPE was observed at the lowest dilution, the titre was defined as 1.80 $\log_{10}$ $TCID_{50}$/mL.

For RNA quantitation by real-time quantitative RT–PCR (RT–qPCR), lung homogenates (100 μL/sample) were placed in 96-well plates and inactivated with 300 μL of TRIzol LS (Thermo Fisher Scientific) for 1 min at room temperature. Total RNA was extracted from the inactivated samples using a Direct-zol-96 RNA Extraction Kit (Zymo Research, Irvine, CA, USA) according to the manufacturer's protocol. The samples were then analysed using a MicroAmp Optical 384-Well Reaction Plate with Barcode (Thermo Fisher Scientific) and Applied Biosystems QuantStudio 5 Real-Time PCR System in conjunction with an EXPRESS One-Step SuperScript qRT–PCR Kit, universal (Thermo Fisher Scientific). The PCR reaction mixes included 2 μL of extracted RNA, 0.4 μM Invitrogen forward primer 2019-nCoV_N1-F (5′-GACCCCAAAATCAGCGAAAT-3′; Thermo Fisher Scientific), 0.4 μM Invitrogen reverse primer 2019-nCoV_N1-R (5′-TCTGGTTACTGCCAGTTGAATCTG-3′; Thermo Fisher Scientific) and 0.25 μM probe 2019-nCoV_N1-P (5′-FAM-ACCCCGCATTACGTTTGGTGGACC-TAMRA-3′; Eurofins, Tokyo, Japan) in total

reaction volumes of 10 μL. The thermal cycling profile included one cycle of 50°C, 15 min; 95°C, 20 s followed by 40 cycles of 95°C, 3 s; 55°C, 30 s. Invitrogen synthetic single-stranded DNA (5′-ATAATGGACCCCAAAATC AGCGAAATGCACCCCGCATTACGTTTGGTGGACCCTCAGATTCAACTGGCAGTAA CCAGAATGGAG-3′; Thermo Fisher Scientific) was 10-fold serially diluted and used to generate a standard curve. The samples were analysed in duplicate.

Evaluation of body weight, lung weight, lung histopathology and nucleocapsid immunohistochemistry

Mouse survival was monitored and body weights recorded at the indicated timepoints. Specifically, 20-week-old mice ($n=5$) infected with the SARS-CoV-2 gamma strain and 40-week-old mice ($n=4$–8) infected with MA-P10 were examined for survival and weighed daily from Day 0 through to Day 14. Whole-lung weight of 40-week-old mice infected with MA-P10 ($n=5$–10) was measured 4 days post-infection. For histopathological analysis, left lungs of 40-week-old mice infected with MA-P10 ($n=3$–5) were fixed in 10% neutral buffered formalin 4 days post-infection, paraffin-embedded, sectioned at 3 μm thickness, and stained with haematoxylin and eosin (H&E). Pathological evaluation was performed by modifying the Owen's report.[7] Blinded histopathological evaluations for alveolar epithelial degeneration or necrosis, bronchial or bronchiolar epithelial degeneration or necrosis, vascular endothelial degeneration or necrosis, alveolar/interstitial inflammation, bronchial or bronchiolar inflammation, perivascular inflammation and thrombosis were independently performed by two pathologists. The lung pathology parameters were scored 0 (normal), 1 (minimal), 2 (mild), 3 (moderate) and 4 (marked). Total histopathological scores for individual mice were calculated by adding the individual histopathological scores, and mean total histopathological scores were calculated for each group. Disparate scores between the pathologists were resolved by the first pathologist rescoring the specimen.

Immunohistochemical (IHC) staining of the left lungs of 40-week-old mice infected with MA-P10 was also performed 4 days post-infection. Briefly, deparaffinized sections were treated with citric acid buffer (pH 6.0) for 10 min at 121°C using an autoclave for antigen retrieval. The sections were incubated with 3% hydrogen peroxide followed by blocking with normal goat serum. The sections were incubated overnight at 4°C with a primary rabbit polyclonal antibody against the SARS-CoV-2 nucleocapsid protein (1:1000; Cat. No. ab281297; Abcam, Cambridge, UK). The sections were then incubated for 30 min at room temperature with a horseradish peroxidase-labelled secondary polyclonal antibody (Cat. No. 414341; Nichirei Biosciences Inc., Tokyo, Japan). The target antigen was detected using 3,3′-diaminobenzidine as a chromogen. The sections were counterstained with haematoxylin and evaluated under a microscope. Semi-quantitative grading of the IHC staining was performed using the following outcomes: –, no staining detected; ±, minimal staining; +, mild staining; ++, moderate staining; +++, marked staining.

Cytokine/chemokine analysis

Cytokine/chemokine levels of TNF-α, IL-1β, IL-6, INF-γ and monocyte chemoattractant protein-1 (MCP-1) were measured in lung homogenates of 40-week-old mice that were non-infected ($n=2$) or infected with MA-P10 and treated twice daily for 3 days with vehicle (MC; $n=3$) or ensitrelvir (8 or 32 mg/kg body weight; $n=5$) starting 24 h post-infection. The lungs were then harvested and homogenates processed 4 days post-infection. Mouse TNF-α Immunoassay (MTA00B), Mouse IL-1β Immunoassay (MLB00C), Mouse IL-6 Immunoassay (M6000B), Mouse INF-γ Immunoassay (MIF00) and Mouse/Rat CCL2/JE/MCP-1 Immunoassay (MJE00B) Quantikine ELISA kits were purchased from R&D Systems (Minneapolis, MN, USA). The assays were performed according to the manufacturer's instructions. The plates were read using an EnSpire microplate reader (PerkinElmer, Waltham, MA, USA) at 450 nm, using 570 nm for correction. The results were quantitated using 4-parameter logistic curve-fit against 2-fold serially diluted standards of each cytokine/chemokine.

Statistical analysis

Statistical analysis was performed using SAS Version 9.4 software (SAS Institute, Cary, NC, USA). The two-sided significance level was set at $P=0.05$. Mean body weight uniformity among the different experimental groups was confirmed by one-way analysis of variance (ANOVA). Endpoint analysis of lung viral titres was measured using a logarithmic scale. To assess ensitrelvir effects on viral titres, the RNA and cytokine/chemokine levels in the lungs of each ensitrelvir-treated group were compared with that of the vehicle-treated group at each timepoint. Dunnett's method was applied to adjust for multiplicity of multiple testing. Survival time comparisons between each ensitrelvir-treated group and the vehicle-treated group were analysed by log-rank test. Proportion comparisons of current body weight to initial body weight between the experimental groups at each timepoint were analysed using one-way ANOVA with equal variance assumption, including the fixed effect of group and contrast method by the analysed timepoints. For mice that died during the experimental period, the proportion of current body weight to initial body weight was imputed at 80% for all timepoints post-death. The fixed-sequence procedure was used to adjust the multiplicity of statistical tests for survival time and body weight analyses.

Results

Effect of ensitrelvir on viral titres and RNA levels in lungs of 5-week-old BALB/cAJcl mice infected with the SARS-CoV-2 gamma strain

To initially evaluate the *in vivo* effect of ensitrelvir on SARS-CoV-2, 5-week-old mice were infected and then orally administered various doses of ensitrelvir or vehicle twice daily starting 24 h post-infection. While all the mice survived, the subsequent analysis revealed that ensitrelvir had a dose-dependent antiviral effect on the viral titres of the SARS-CoV-2 gamma strain in the lungs of infected mice [Figure 1(a)]. Both 32 and 64 mg/kg ensitrelvir treatments resulted in significant reduction of viral titres 2 and 3 days post-infection as compared with that of vehicle treatments ($P<0.0001$). In addition, 8 and 16 mg/kg ensitrelvir treatments significantly reduced lung viral titres at 3 days post-infection ($P<0.05$ and $P<0.01$, respectively). Likewise, ensitrelvir dose-dependently reduced viral RNA levels of the SARS-CoV-2 gamma strain [Figure 1(b), Table S1, available as Supplementary data at *JAC* Online]. Compared with the vehicle-treated group, treatment with ensitrelvir significantly reduced the amount of viral RNA in the lungs of infected mice 2 and 3 days post-infection at doses of 16 mg/kg ($P<0.01$ and $P<0.05$, respectively), 32 mg/kg ($P<0.01$ and $P<0.0001$, respectively) and 64 mg/kg ($P<0.0001$ and $P<0.0001$, respectively). A significant reduction was also observed with 8 mg/kg ensitrelvir treatment as compared with the vehicle-treated group at 3 days post-infection ($P<0.05$). When 5-week-old BALB/c mice were infected with 5 $\log_{10}$ $TCID_{50}$ of the SARS-CoV-2 gamma strain, their body weight declined to approximately 90% of their original mass on Day 3 or 4 post-infection, which was quickly recovered (data not shown).

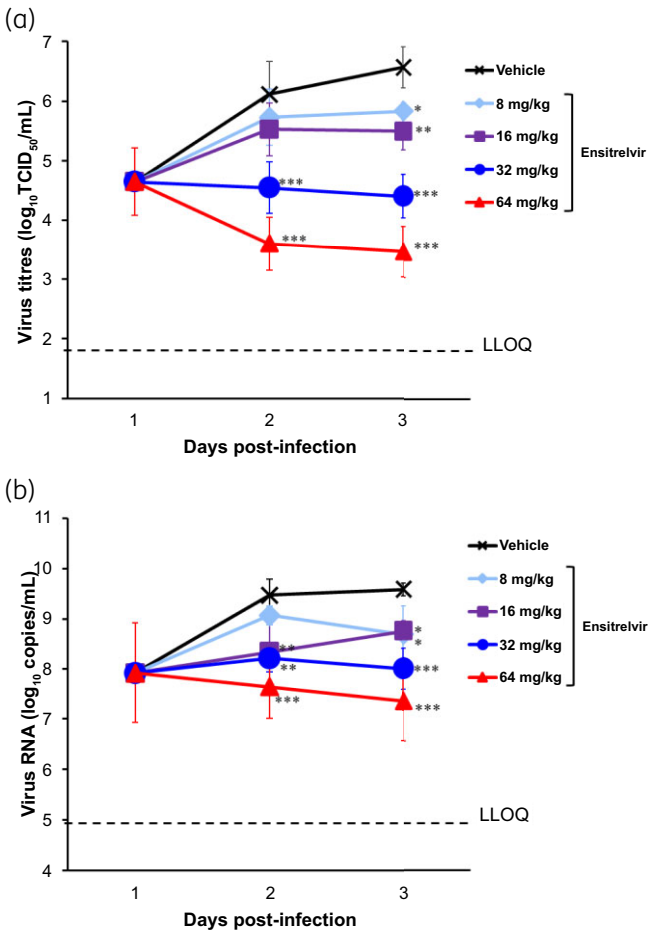

Figure 1. Effect of ensitrelvir on viral titres and RNA levels in 5-week-old female BALB/cAJcl mice infected with the SARS-CoV-2 gamma strain (hCoV-19/Japan/TY7-501/2021). The mice were nasally infected with SARS-CoV-2 and then orally administered various doses of ensitrelvir or vehicle (0.5% MC solution) every 12 h (twice daily) for 2 days. The first administration was performed 24 h post-infection. (a) Viral titres in lungs of mice were determined using VeroE6/TMPRSS2 cells. Each point represents the mean ± SD of five mice. The dashed line represents the lower limit of quantification (LLOQ; 1.80 $\log_{10}$ $TCID_{50}$/mL). *P* values were calculated by Dunnett's method versus vehicle. **P* < 0.05, ***P* < 0.01, ****P* < 0.0001. (b) Viral RNA levels in the lungs of mice were determined using RT–qPCR. Each point represents the mean ± SD of five mice. The dashed line represents the LLOQ (4.92 $\log_{10}$ copies/mL). *P* values were calculated by Dunnett's method versus vehicle. **P* < 0.05, ***P* < 0.01, ****P* < 0.0001.

Effect of ensitrelvir on body weight of 20-week-old BALB/cAJcl mice infected with the SARS-CoV-2 gamma strain

Host factors, including age, are key determinants of disease severity and progression for COVID-19, both in humans[8] and mice.[6,9] Therefore, we evaluated the effect of ensitrelvir in older (20-week-old) mice infected with SARS-CoV-2. As an indicator of disease progression, the mice were monitored for body weight loss caused by infection with the SARS-CoV-2 gamma strain (Figure 2). Body weight loss was observed in vehicle-treated mice infected with the SARS-CoV-2 gamma strain starting at 3 days post-infection; however, the weight loss was significantly

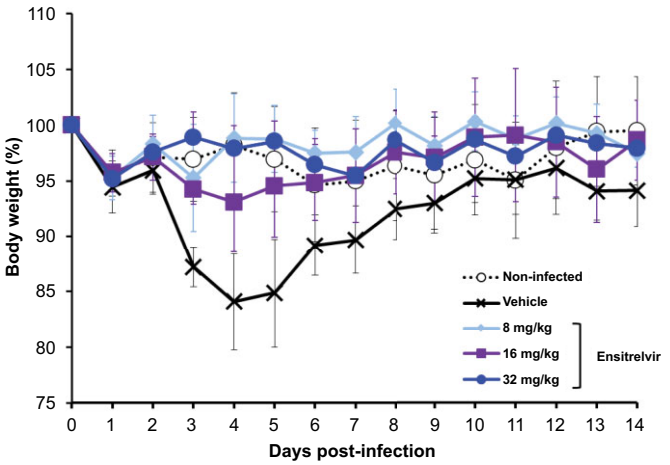

Figure 2. Effect of ensitrelvir on the body weight of 20-week-old female BALB/cAJcl mice infected with the SARS-CoV-2 gamma strain (hCoV-19/Japan/TY7-501/2021). The mice were nasally infected with SARS-CoV-2 and then orally administered various doses of ensitrelvir or vehicle (0.5% MC solution) every 12 h (twice daily) for 5 days. The first administration was performed 24 h post-infection. Results are presented as the percentage of current body weight as compared with that of initial body weight prior to infection. Each point represents the mean ± SD of five mice.

suppressed from 3 to 8 days post-infection with administration of ≥8 mg/kg ensitrelvir (*P* < 0.05). Furthermore, the body weight of ensitrelvir-treated mice was not significantly different from that of non-infected control mice. No mortality was observed in any of the experimental groups.

Effect of ensitrelvir on 40-week-old BALB/cAJcl mice infected with SARS-CoV-2 MA-P10

To further increase the severity of SARS-CoV-2 infection in our test system, we used aged (retired; 40-week-old) mice infected with the mouse-adapted SARS-CoV-2 MA-P10 strain. Infected mice were orally administered various doses of ensitrelvir or vehicle twice daily for 5 days starting 24 h post-infection. The mice were then monitored for survival and body weight loss. The results showed that ensitrelvir improved the survival rates of mice in a dose-dependent manner [Figure 3(a)]. While improved survival was not observed with 4 mg/kg ensitrelvir as compared with that of vehicle-treated mice, survival time significantly improved for infected mice treated with 8 mg/kg (*P* < 0.05), 16 mg/kg (*P* < 0.001) and 32 mg/kg (*P* < 0.001) ensitrelvir. Ensitrelvir treatment also suppressed the body weight loss observed in mice treated with vehicle and did so in a dose-dependent manner [Figure 3(b)]. Significant protection from body weight loss compared with that of the vehicle-treated group was observed 2 days post-infection with 32 mg/kg ensitrelvir (*P* < 0.01), 3 days post-infection with 16 mg/kg (*P* < 0.01) and 32 mg/kg (*P* < 0.001) ensitrelvir, and 4 and 5 days post-infection with 8 mg/kg (*P* < 0.01), 16 mg/kg (*P* < 0.001) and 32 mg/kg (*P* < 0.001) ensitrelvir.

Ensitrelvir also effectively reduced MA-P10 titres in the lungs of infected 40-week-old mice [Figure 4(a), Table S2]. Ensitrelvir

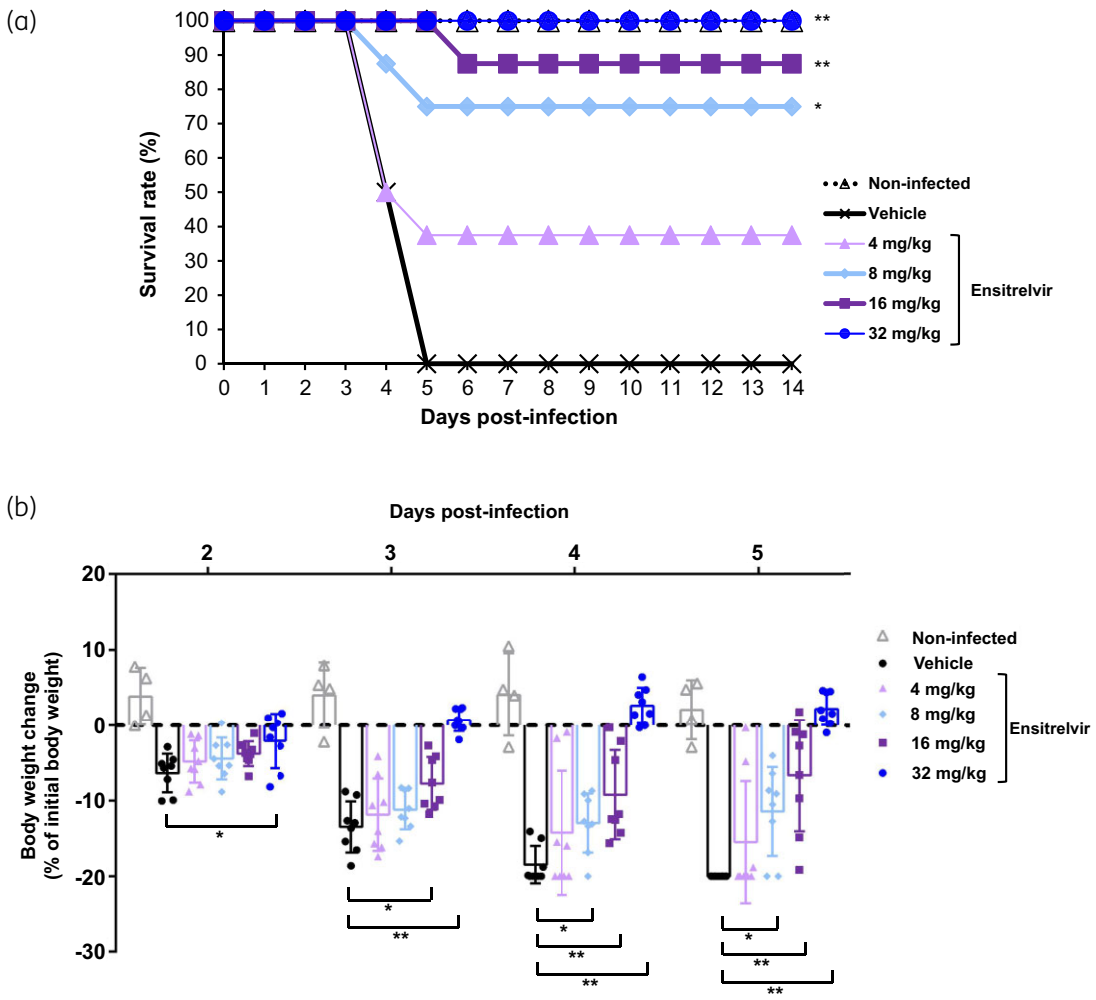

Figure 3. Effect of ensitrelvir on survival and the body weight of 40-week-old female BALB/cAJcl mice infected with mouse-adapted SARS-CoV-2 MA-P10. The mice were nasally infected with SARS-CoV-2 and then orally administered various doses of ensitrelvir or vehicle (0.5% MC solution) every 12 h (twice daily) for 5 days. The first administration was performed 24 h post-infection. (a) Mouse survival was monitored daily, and survival curves generated using Kaplan–Meier analysis. There were four mice/group for non-infected mice and eight mice/group for infected mice. *P* values were calculated using log-rank test versus vehicle (multiplicity was adjusted by fixed-sequence procedure). $^{*}P < 0.05$ and $^{**}P < 0.001$. (b) Body weight values are presented as a percentage of initial body weight for Days 2–5 post-infection. The graph bars represent the mean ± SD of four mice/group for non-infected mice and eight mice/group for infected mice. *P* values were calculated using ANOVA test versus vehicle (multiplicity was adjusted by fixed-sequence procedure). $^{*}P < 0.01$ and $^{**}P < 0.001$.

treatment at 8 mg/kg significantly reduced lung viral titres compared with that of vehicle treatment at 4 days post-infection ($P < 0.05$), while treatment with 32 mg/kg ensitrelvir reduced viral levels at 2 days ($P < 0.01$), 3 days ($P < 0.0001$) and 4 days ($P < 0.0001$) post-infection. This *in vivo* activity was consistent with the *in vitro* effect of ensitrelvir inhibiting CPE in MA-P10-infected VeroE6/TMPRSS2 cells (detailed methods for the *in vitro* viral replication inhibition assays are described in the Supplementary data). Briefly, the mean EC_{50} of ensitrelvir against MA-P10 ± standard deviation (SD), based on three independent experiments, was 0.12 ± 0.04 μmol/L compared with that of 1.6 ± 0.1 μmol/L for remdesivir.

Treatment of SARS-CoV-2 MA-P10-infected 40-week-old mice 24 h post-infection with ensitrelvir also resulted in dose-dependent suppression of inflammatory cytokine/chemokine production 4 days post-infection, including TNF-α, IL-1β, IL-6 and MCP-1 [Figure 4(b)]. Ensitrelvir at a dose of 32 mg/kg restored the levels of all the cytokines examined to those at or near levels observed in non-infected mice. In a previous study, the lung weight of mice increased following influenza virus infection, along with increased infiltration of inflammatory cells.[10] Therefore, we analysed the lung weight of SARS-CoV-2 MA-P-10-infected mice in the current study and found it had increased compared with that of non-infected mice. However, treatment with 32 mg/kg ensitrelvir significantly suppressed the lung weight increases 4 days post-infection as compared with that of vehicle-treated mice [Figure 4(c)]. Furthermore, at 4 days post-infection, TNF-α, IL-6 and MCP-1 levels positively

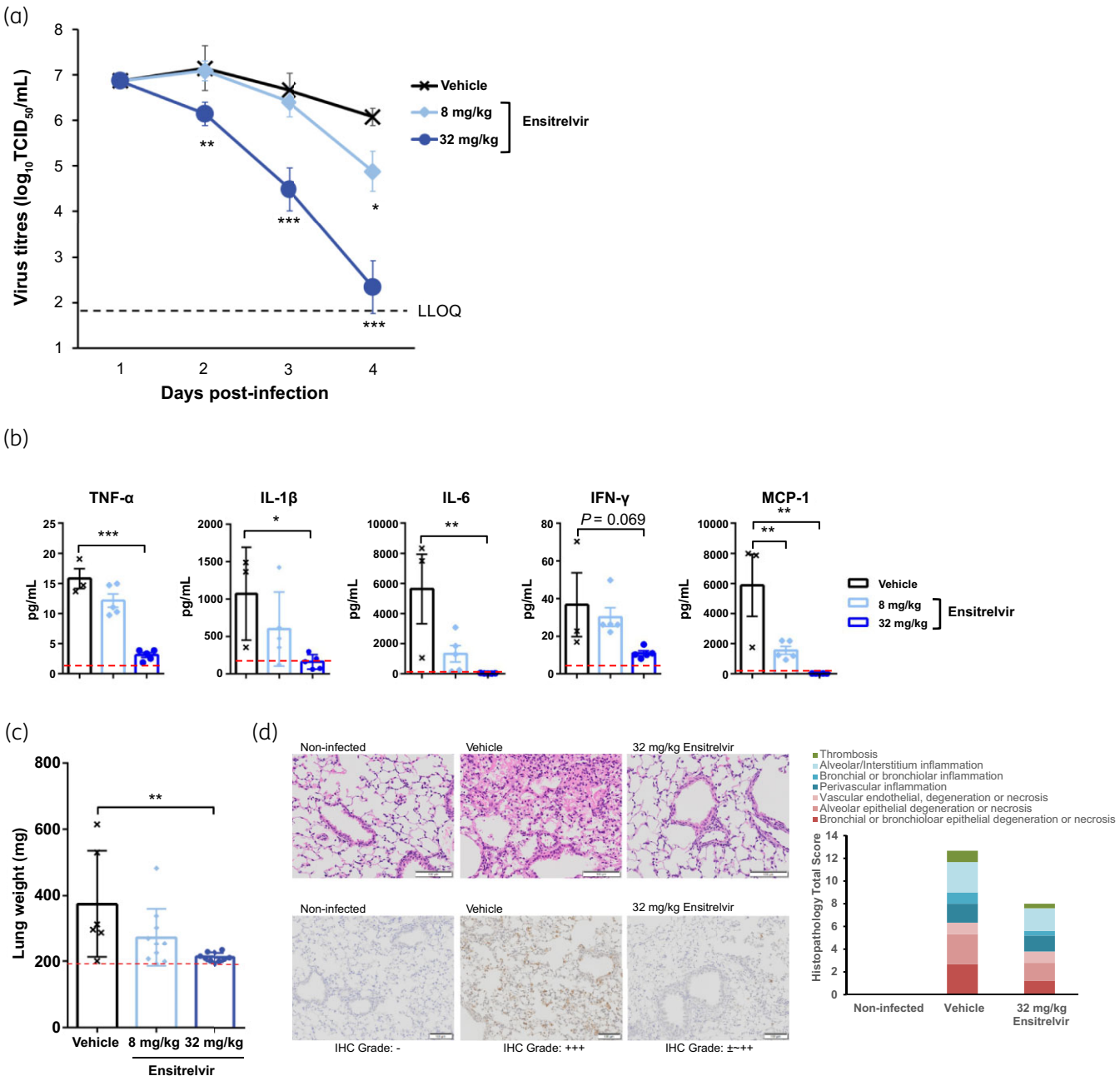

Figure 4. Effect of ensitrelvir on viral titre, cytokine/chemokine production, lung weight and lung pathology in 40-week-old female BALB/cAJcl mice infected with mouse-adapted SARS-CoV-2 MA-P10. The mice were infected with SARS-CoV-2 and then orally administered various doses of ensitrelvir or vehicle (0.5% MC solution) every 12 h (twice daily) for 3 days. The first administration was performed 24 h post-infection. (a) Viral titres in the lungs were determined using VeroE6/TMPRSS2 cells. Each point represents the mean ± SD. The dashed line represents an LLOQ of 1.80 $\log_{10}$ TCID$_{50}$/mL. *P* values were calculated by Dunnett's method versus vehicle. $^{*}P<0.05$, $^{**}P<0.01$, $^{***}P<0.0001$. There were five mice/group except for Day 4 of the vehicle-treated group, for which there were three mice/group. (b) Cytokine/chemokine levels in mouse lungs 4 days post-infection were determined using ELISA assays. The red lines indicate cytokine/chemokine levels detected in non-infected control mice ($n=2$). The graph bars represent the mean ± SD. *P* values were calculated by Dunnett's multiple comparison test versus vehicle. $^{*}P<0.05$, $^{**}P<0.01$, $^{***}P<0.001$. There were five mice/group except for the vehicle-treated group, for which there were 3 mice/group. (c) Lung weight of vehicle-treated ($n=6$) and ensitrelvir-treated (8 and 32 mg/kg) ($n=10$) mice 4 days post-infection. The red lines indicate lung weight of non-infected control mice ($n=3$). The graph bars represent the mean ± SD. *P* values were calculated by Dunnett's method versus vehicle. $^{**}P<0.01$. (d) Histopathology of the lung assessed by H&E staining (upper panels) and IHC staining of viral nucleocapsid (lower panels). Mice treated with 32 mg/kg ensitrelvir ($n=3$) exhibited less lung pathology and reduced IHC staining for virus capsid as compared with that of the vehicle-treated group ($n=5$). Non-infected control mice ($n=3$) were negative for IHC staining. IHC grade: –, not detected; ±, minimal; +, mild; ++, moderate; +++, marked. Data from dead mice were excluded from the analysis.

correlated with the viral titres, and IL-1β, IL-6 and MCP-1 levels positively correlated with the lung weights (Figure S1).

Consistent with the cytokine/chemokine and lung weight results, lung histopathology revealed degeneration and necrosis of alveolar, bronchial or bronchiolar epithelium cells and vascular endothelial cells, as well as the presence of inflammation and thrombus, in vehicle-treated mice infected with SARS-CoV-2 MA-P-10 [Figure 4(d)]. In contrast, the severity of these infection-related pulmonary lesions was reduced in mice treated with 32 mg/kg ensitrelvir starting 24 h post-infection. Furthermore, the amount of positive immunostaining for virus nucleocapsid was reduced in MA-P10-infected mice treated with 32 mg/kg ensitrelvir as compared with that of vehicle-treated mice.

Discussion

The current study demonstrated that ensitrelvir reduced SARS-CoV-2 virus levels in a dose-dependent manner compared with that of vehicle treatments, as indicated by infectious viral titres and viral RNA levels in the lungs of infected mice. Furthermore, the antiviral activity correlated with increased survival, reduced body weight loss, reduced pulmonary lesions and suppression of inflammatory cytokine/chemokine levels. Importantly, the observed *in vivo* effects of ensitrelvir occurred in a delayed-treatment model system. Ensitrelvir shows high selectivity against the 3CL protease[4] and the body weight changes of infected mice were similar to that of non-infected mice administered 32 mg/kg ensitrelvir. Accordingly, no ensitrelvir-associated toxicity was observed in the mice of this study.

Ensitrelvir is an inhibitor of the SARS-CoV-2 3CL protease, which is essential for processing of the SARS-CoV-2-encoded polyprotein, as well as viral replication.[11] The 3CL proteases of SARS-CoV-2 and other coronaviruses, such as feline infectious peritonitis virus and porcine deltacoronavirus, are known to antagonize innate immune function, including the inhibition of type I IFN signalling and participation in the TGF-β signalling pathway.[12–14] Furthermore, the 3CL protease-mediated cleavage of NLRP12 may explain the hyperinflammatory response observed in patients with severe COVID-19.[15,16] Elevated IL-6 levels have also been correlated with increased mortality in patients with COVID-19.[17] Thus, the findings in the current study of ensitrelvir repressing IL-6 expression may suggest its potential for reducing mortality in patients with COVID-19. The 3CL protease is an ideal antiviral target for SARS-CoV-2, its variants and potential future viruses as it is conserved among coronaviruses. Moreover, it plays a critical role in viral replication, yet there are no known human host-cell proteases with the same substrate specificity.[11]

According to a previous report, patients with COVID-19 have significantly elevated levels of inflammatory markers, such as IL-1β and IFNγ.[18] In addition, the concentration of MCP-1 and TNF-α in patients with severe illness are higher than those in patients with mild COVID-19,[18] suggesting that cytokine storms contribute to disease severity. Moreover, elevated levels of these inflammatory markers were also observed in mouse lungs using our infection model, but their expression was suppressed by ensitrelvir treatment. The positive correlation between inflammatory markers and viral titres suggests that ensitrelvir, through its antiviral effect, is able to suppress the production of components of the cytokine storm caused by SARS-CoV-2 infection, thus imparting a protective effect on lung structure.

Small-animal models that recapitulate SARS-CoV-2 infection and disease are critical for studying COVID-19 and for evaluating potential vaccines and therapeutics. The use of mice and mouse-adapted virus strains as model systems has been previously documented.[6,9] Our current findings also demonstrate the utility of the model for SARS-CoV-2 replication, infection and pathogenesis studies, thus making it a powerful resource for evaluating the efficacy of antivirals against SARS-CoV-2 and in preventing COVID-19 progression. Nirmatrelvir, another 3CL protease inhibitor, shows antiviral activity in a mice model when treatment is started 4 h post-infection.[7] In the current study, ensitrelvir also showed antiviral activity in a delayed-treatment mouse model. This suggests that 3CL protease inhibitors are effective against SARS-CoV-2 in mice, even after the initiation of infection. We would like to directly compare these two compounds in future studies.

The current study did have certain limitations. For instance, differences do exist between humans and mice. Importantly, ensitrelvir exhibits lower clearance and longer half-lives in non-rodents compared with that in rodents.[4] Accordingly, we performed twice-daily administration of ensitrelvir to the mice, while once-daily administration is expected in clinical treatment. Furthermore, while evaluation of ensitrelvir included both a SARS-CoV-2 gamma and a mouse-adapted strain, no direct evidence was provided regarding its efficacy against other SARS-CoV-2 variants. However, conservation of 3CL proteases and their importance in the virus life cycle suggest that the *in vivo* efficacy of ensitrelvir is likely against a broad range of SARS-CoV-2 strains, as well as potentially against other coronaviruses. However, this hypothesis remains to be comprehensively investigated.

In conclusion, this study was the first evaluation of the *in vivo* efficacy in a delayed-treatment mouse model of the antiviral ensitrelvir, which is under clinical development. The development of safe and effective antiviral therapies is essential in combating the worldwide health threat of COVID-19, as well as future threats posed by novel coronaviruses. The current findings suggest that ensitrelvir has the potential to suppress viral replication and the aggravation of clinical disease caused by SARS-CoV-2 infection, which is important as SARS-CoV-2 is now a human pathogen with worldwide distribution. The results justify the continued clinical development of ensitrelvir as a potent antiviral treatment for SARS-CoV-2 infections.

Acknowledgements

Portions of the reported findings were presented at the Annual meeting of Japanese Association for Infectious Diseases in April 2022.

We acknowledge the National Institute of Infectious Diseases (NIID) for providing the SARS-CoV-2 gamma strain (hCoV-19/Japan/TY7-501/2021). We also acknowledge Prof. Hirofumi Sawa (Hokkaido University, Sapporo, Japan) for providing the SARS-CoV-2 MA-P10 strain. We are grateful to all our colleagues who participated in the COVID-19 antiviral programme at Shionogi and thank Shionogi Techno-Advance Research Co., Ltd. for technical support in the pharmacological studies. Editorial support in the form of medical writing and creating high-resolution images based on the authors' detailed directions, collating author

comments, copyediting, fact checking and referencing was provided by Editage, Cactus Communications.

Funding

This work was supported by internal funding from Shionogi & Co., Ltd. The editorial support provided by Editage was also funded by Shionogi & Co., Ltd.

Transparency declarations

All authors are employees of Shionogi & Co., Ltd. and a subsidiary company.

Supplementary data

Supplementary Methods, Figure S1 and Tables S1 and S2 are available as Supplementary data at *JAC* Online.

References

1 WHO. Weekly epidemiological update on COVID-19 - 15 March 2022. Edition 83. https://www.who.int/publications/m/item/weekly-epidemiological-update-on-covid-19—15-march-2022.

2 Helmy YA, Fawzy M, Elaswad A *et al.* The COVID-19 pandemic: a comprehensive review of taxonomy, genetics, epidemiology, diagnosis, treatment, and control. *J Clin Med* 2020; **9**: 1225. https://doi.org/10.3390/jcm9041225

3 Izda V, Jeffries MA, Sawalha AH. COVID-19: a review of therapeutic strategies and vaccine candidates. *Clin Immunol* 2021; **222**: 108364. https://doi.org/10.1016/j.clim.2020.108634

4 Unoh Y, Uehara S, Nakahara K *et al.* Discovery of S-217622, a non-covalent oral SARS-CoV-2 3CL protease inhibitor clinical candidate for treating COVID-19. *J Med Chem* 2022; **65**: 6499–512. https://doi.org/10.1021/acs.jmedchem.2c00117

5 Matsuyama S, Nao N, Shirato K *et al.* Enhanced isolation of SARS-CoV-2 by TMPRSS2-expressing cells. *Proc Nat Acad Sci U S A* 2020; **117**: 7001–3. https://doi.org/10.1073/pnas.2002589117

6 Gu H, Chen Q, Yang G *et al.* Adaptation of SARS-CoV-2 in BALB/c mice for testing vaccine efficacy. *Science* 2020; **369**: 1603–7. https://doi.org/10.1126/science.abc4730

7 Owen DR, Allerton CMN, Anderson AS *et al.* An oral SARS-CoV-2 M^{pro} inhibitor clinical candidate for the treatment of COVID-19. *Science* 2021; **374**: 1586–93. https://doi.org/10.1126/science.abl4784

8 Chen Y, Klein SL, Garibaldi BT *et al.* Aging in COVID-19: vulnerability, immunity and intervention. *Aging Res Rev* 2021; **65**: 101205. https://doi.org/10.1016/j.arr.2020.101205

9 Sun S, Gu H, Cao L *et al.* Characterization and structural basis of a lethal mouse-adapted SARS-CoV-2. *Nat Comm* 2021; **12**: 5654. https://doi.org/10.1038/s41467-021-25903-x

10 Fukao K, Noshi T, Yamamoto A *et al.* Combination treatment with the cap-dependent endonuclease inhibitor baloxavir marboxil and a neuraminidase inhibitor in a mouse model of influenza A virus infection. *J Antimicrob Chemother* 2019; **74**: 654–62. https://doi.org/10.1093/jac/dky462

11 Ullrich S, Nitsche C. The SARS-CoV-2 main protease as drug target. *Bioorg Med Chem Lett* 2020; **30**: 127377. https://doi.org/10.1016/j.bmcl.2020.127377

12 Moustaqil M, Ollivier E, Chiu H-P *et al.* SARS-CoV-2 proteases PLpro and 3CLpro cleave IRF3 and critical modulators of inflammatory pathways (NLRP12 and TAB1): implications for disease presentation across species. *Emerg Microbes Infect* 2021; **10**: 178–95. https://doi.org/10.1080/22221751.2020.1870414

13 Chen S, Tian J, Li Z *et al.* Feline infectious peritonitis virus Nsp5 inhibits type I interferon production by cleaving NEMO at multiple sites. *Viruses* 2019; **12**: 43. https://doi.org/10.3390/v12010043

14 Zhu X, Chen J, Tian L *et al.* Porcine deltacoronavirus nsp5 cleaves DCP1A to decrease its antiviral activity. *J Virol* 2020; **94**: e02162-19. https://doi.org/10.1128/JVI.02162-19

15 Chen G, Wu D, Guo W *et al.* Clinical and immunological features of severe and moderate coronavirus disease 2019. *J Clin Invest* 2020; **130**: 2620–9. https://doi.org/10.1172/JCI137244

16 Giamarellos-Bourboulis EJ, Netea MG, Rovina N *et al.* Complex immune dysregulation in COVID-19 patients with severe respiratory failure. *Cell Host Microbe* 2020; **27**: 992–1000.e3. https://doi.org/10.1016/j.chom.2020.04.009

17 Zhou F, Yu T, Du R *et al.* Clinical course and risk factors for mortality of adult inpatients with COVID-19 in Wuhan, China: a retrospective cohort study. *Lancet* 2020; **395**: 1054–62. https://doi.org/10.1016/S0140-6736(20)30566-3

18 Huang C, Wang Y, Li X *et al.* Clinical features of patients infected with 2019 novel coronavirus in Wuhan, China. *Lancet* 2020; **395**: 497–506. https://doi.org/10.1016/S0140-6736(20)30183-5